NASA-CR-204838

Ind. Eng. Chem. Res. **1996,** *35,* 1078–1084

Metastable Solution Thermodynamic Properties and Crystal Growth Kinetics

Soojin Kim and Allan S. Myerson*,†

Department of Chemical Engineering, Polytechnic University, Six Metrotech Center, Brooklyn, New York 11201

The crystal growth rates of $NH_4H_2PO_4$, KH_2PO_4, $(NH_4)_2SO_4$, $KAl(SO_4)_2 \cdot 12H_2O$, NaCl, and gl and the nucleation rates of KBr, KCl, $NaBr \cdot 2H_2O$, $(NH_4)_2Cl$, and $(NH_4)_2SO_4$ were express d terms of the fundamental driving force of crystallization calculated from the activi y supersaturated solutions. The kinetic parameters were compared with those from the comm o used kinetic expression based on the concentration difference. From the viewpoi t thermodynamics, rate expressions based on the chemical potential difference provide accu r kinetic representation over a broad range of supersaturation. The rates estimated usin expression based on the concentration difference coincide with the true rates of crystalliz ti only in the concentration range of low supersaturation and deviate from the true kineti s the supersaturation increases.

Introduction

Crystallization is an important separation and purification process used in many areas such as the chemical, pharmaceutical, petrochemical, and electronics industries. The kinetics of crystallization is essential information required for the design of any crystallization equipment. Numerous experimental works investigating the kinetics of crystal growth and nucleation have been published in the literature. However, a standardized approach in correlating experimental results to the theoretical or semiempirical models to describe the kinetic processes has not been established. Consequently, estimating rates of crystallization from different expressions often leads to inconsistent results.

The driving force for crystallization is the degree of supersaturation which has been commonly expressed, for the sake of convenience, as the difference in concentration between the supersaturated and saturated solutions. This practice of expressing the crystallization rate as a function of the concentration difference causes confusion and inconsistency: even dimensionless supersaturations calculated from different concentration units result in different numerical values that are not proportional to one another, and thus different sets of kinetic parameters could be evaluated from a given set of experimental data.

It is well-known that the fundamental driving force of crystallization is the difference between the chemical potential of the supersaturated solution and that of the solid crystal face, which can be used independently of units (Mullin and Söhnel, 1977). Using the concentration difference in place of the fundamental driving force of crystallization is based on the assumption that the solute activity coefficient of a supersaturated solution can be closely approximated by that of the saturated solution, which may cause serious errors in evaluating the true kinetics of crystallization.

Unfortunately, the kinetic expression using the fundamental driving force seldom has been used in crystallization practices, because there had been virtually no experimental data of activity in supersaturated solutions. Recently, efforts to study thermodynamic properties of supersaturated solutions have been carried out by a number of researchers utilizing an electrodynamic microparticle levitator (Cohen et al., 1987; Na, 199 et al., 1994, 1995). Water activities of many aqu supersaturated solutions have been measured usi single micron-sized solution droplet that is electri a levitated and continuously weighed as the concentr ti is increased by a slow evaporation of water. S l activity of the supersaturated solutions can be comp at from the water activity data using the Gibbs–Du e relation; hence, we can establish a direct relatio sl between the chemical potential and the concentra ti of a supersaturated solution.

From this relationship, many kinetic data rep i in the literature can now be expressed in terms o t chemical potential difference providing kinetic exp r sions of more exact and thermodynamically acc a form. The purpose of this paper is to investigate t effects of using the fundamental driving force in t expression of crystallization kinetics and to quantif t errors associated with the conventional use of t concentration-based driving force on the actual rat s crystallization.

Theoretical Section

Driving Force for Crystallization. The fu mental driving force for crystallization can be expre s in dimensionless form:

$$(\mu - \mu^*)/RT = \ln(a/a^*)$$

For electrolyte solutions, the driving force is expre s in terms of the mean ionic activity of the solute, a

$$\frac{\mu - \mu^*}{RT} = \nu \ln\left(\frac{a_\pm}{a_\pm{}^*}\right) = \nu \ln\left(\frac{\gamma_\pm}{\gamma_\pm{}^*}\frac{c}{c^*}\right)$$

where c is the concentration and $\gamma_\pm$ is the correspon mean ionic activity coefficient. The fundamenta mensionless driving force for an electrolyte solution v demonstrated to be the same whether the salt dis o ates partially or totally in solution (Söhnel and Mu l 1978). For solutions of hydrate salts, the term μ refers to the chemical potential difference between hydrate in supersaturated and saturated soluti n respectively, even though the existence of a hydrat solution may be only hypothetical (Söhnel and Mu l 1978).

† e-mail: amyerson@roebling.poly.edu. Fax: (718) 260-3776.

0888-5885/96/2635-1078$12.00/0 © 1996 American Chemical Society

The use of the dimensionless concentration difference

$$\sigma = (c - c^*)/c^* \tag{3}$$

as the driving force in place of $\Delta\mu/RT$ is justified only in the case that meets the following conditions: (i) $\gamma_\pm \approx \gamma_\pm^*$, thus $\ln(a_\pm/a_\pm^*) \approx \ln(c/c^*)$; (ii) $\sigma \ll 1$, thus $\ln(\sigma + 1) \approx \sigma$, and (iii) $\nu = 1$.

Condition i will be satisfied only for an ideal solution or for a solution whose supersaturation is small enough so that its concentration is almost the same as that of the saturated solution. There are many circumstances in crystallization practices in which a high supersaturation level ($\sigma > 0.1$, for example) is encountered and thus condition ii is violated. Examples are primary nucleation and precipitation processes where relatively insoluble materials are produced as a result of reaction. Condition iii will be met for only nondissociating salts and hence is inapplicable for electrolytes. Therefore, using σ in place of $\Delta\mu/RT$ is an approximation that is inadequate in a number of practical situations.

Solute Activity. Solute activity is computed from experimental water activity data as a function of concentration. Through the Gibbs–Duhem equation relating the chemical potentials of solvent and solute at constant temperature and pressure, the water activity can be expressed in terms of solute concentration, m in molality, for example (Robinson and Stokes, 1959):

$$-(1000/\mathrm{MW_w})\, \mathrm{d}(\ln a_w) = \nu m\, \mathrm{d}(\ln(\gamma_\pm m)) \tag{4}$$

upon integration of which we get the relation:

$$\ln(\gamma_\pm/\gamma_\pm^*) = \phi - \phi^* + \int_{m^*}^{m} \frac{\phi - 1}{m}\, \mathrm{d}m \tag{5}$$

where ϕ, the osmotic coefficient, is defined as

$$\phi = -\frac{1000}{\mathrm{MW_w}} \frac{\ln a_w}{\nu m}$$

Therefore,

$$\ln(a_\pm/a_\pm^*) = \ln(m/m^*) + \phi - \phi^* + \int_{m^*}^{m} \frac{\phi - 1}{m}\, \mathrm{d}m \tag{6}$$

Crystallization Kinetics. a. Power Law Expression. For correlation purposes, a simple semiempirical power law equation of the form

$$G = k\sigma^n \tag{7}$$

has been used frequently for the expression of surface integration rate of crystal growth and nucleation rate. The kinetic expression in terms of the fundamental dimensionless driving force, as shown in eq 2, is:

$$G = k'\left(\frac{\Delta\mu}{RT}\right)^{n'} = k'\left(\nu \ln\left(\frac{a_\pm}{a_\pm^*}\right)\right)^{n'} = k'\left(\nu \ln\left(\frac{\gamma_\pm}{\gamma_\pm^*}\frac{m}{m^*}\right)\right)^{n'} \tag{8}$$

The kinetic orders n and n' would be the same only in the concentration range of very low supersaturations, where $\gamma_\pm/\gamma_\pm^* \approx 1$ and $\ln(\sigma + 1)$ can be approximated as σ. The difference between experimentally obtained n and n' will be greater for the data of a kinetic experiment conducted at a higher supersaturation range. Thermodynamically, the surface integration rate of crystal growth is determined by the constant power of the fundamental driving force; therefore, true kinetics of crystallization can be described by eq 8 only. The kinetic expression (eq 7) based on constant parameters, k and n, is applicable only in the restricted range of σ in which the experimental data were obtained to determine the parameters and cannot be used for the prediction of crystallization rates over a broader range of concentration.

The power law correlation, eq 8, is used here to represent the process occurring at the crystal surface only. Therefore, the validity of the equation is limited by the assumption that the solute concentration at the crystal surface is equal to the bulk concentration especially at high supersaturation where the effect of the mass transfer diffusion resistance is relatively large.

b. Boundary Layer Diffusion Model. The overall rate of crystal growth determined both by the mass-transfer rate of solute diffusion and by surface integration to the crystal lattice has been described in terms of the concentration-based driving forces:

$$R_g = k_d \frac{c - c_i}{c^*} = k_r \left(\frac{c_i - c^*}{c^*}\right)^n \tag{9}$$

where c_i is the interface concentration and can be eliminated to give

$$R_g = k_r \left(\frac{c - c^*}{c^*} - \frac{R_g}{k_d}\right)^n \tag{10}$$

which is often numerically evaluated. Equations 9 and 10 are valid only in a narrow range of concentration. Thermodynamically exact overall growth rate can be written as:

$$R_g = k_d' \frac{\mu - \mu_i}{RT} = k_r' \left(\frac{\mu_i - \mu^*}{RT}\right)^{n'} \tag{11}$$

or

$$R_g = k_d' \nu \ln(a_\pm/a_{\pm i}) = k_r' \nu \ln(a_\pm/a_\pm^*)^{n'} \tag{12}$$

where μ_i is the chemical potential at the interface. Analogously to eq 10, the overall growth rate, R_g, can be evaluated numerically by eliminating the interface solute activity, $a_{\pm i}$. This overall growth rate, R_g, expressed as a function of the chemical potential difference, presents the true kinetics of growth over a wide range of concentration.

Results and Discussion

Kinetics of Crystal Growth. a. Surface Integration Kinetics. Experimental data of the crystal growth rates of $NH_4H_2PO_4$, KH_2PO_4, $(NH_4)_2SO_4$, $KAl(SO_4)_2 \cdot 12H_2O$, and NaCl at 25 °C and of glycine at 20 °C are reported in the literature (Mullin and Amatavivadhana, 1967a,b; Mullin et al., 1970; Mullin and Garside, 1967; Rumford and Bain, 1960; Li and Rodríguez-Hornedo, 1992). These authors had conducted the kinetic experiments using fairly high solution velocity in order to eliminate diffusional mass-transfer resistance and thus to measure the surface integration rates. First, the supersaturation data expressed in various units in different papers were converted to be in a consistent unit of molality (mol of solute/kg of water or mol of hydrate/kg of "free" water). The data of growth rates were converted to contain the unit of kg of crystal/(m^2 of surface area·s).

The water activity data of NaCl, $(NH_4)_2SO_4$, and glycine solutions reported by Cohen et al. (1987) and

Table 1. Coefficients of $a_w(m)$ from the Polynomial $a_w = a_0 + a_1m + a_2m^2 + ...$[a] at 20–25 °C

salt	a_0	a_1	a_2	a_3	a_4	a_5	a_6	m range of validit
$NH_4H_2PO_4$	1.0726	-3.081×10^{-2}	4.828×10^{-4}	-4.008×10^{-6}	1.629×10^{-8}	-2.527×10^{-11}	0	3.4–60
KH_2PO_4	0.9777	-1.762×10^{-2}	-1.387×10^{-3}	9.390×10^{-5}	-2.128×10^{-6}	1.669×10^{-8}	0	1.6–20
$KAl(SO_4)_2 \cdot 12H_2O$[b]	1.0400	-1.702×10^{-1}	2.788×10^{-2}	-2.443×10^{-3}	1.055×10^{-4}	-1.757×10^{-6}	0	0.2–20
$(NH_4)_2SO_4$	0.9968	-2.969×10^{-2}	1.753×10^{-5}	-3.253×10^{-4}	3.571×10^{-5}	-9.787×10^{-7}	0	0.1–18
NaCl	1.0084	-4.939×10^{-2}	8.888×10^{-3}	-2.157×10^{-3}	1.617×10^{-4}	-1.990×10^{-6}	-1.142×10^{-7}	0.5–14
glycine	1.0089	-3.081×10^{-2}	4.828×10^{-4}	-4.008×10^{-6}	1.629×10^{-8}	-2.527×10^{-11}	0	3.3–25
KBr	1.0008	-3.531×10^{-2}	2.490×10^{-3}	-6.729×10^{-4}	5.318×10^{-5}	-8.040×10^{-7}	-2.866×10^{-8}	0.1–15
KCl	0.9975	-2.173×10^{-2}	-1.053×10^{-2}	4.253×10^{-3}	-7.780×10^{-4}	6.203×10^{-5}	-1.764×10^{-6}	0.1–13
NH_4Cl	0.9968	-2.611×10^{-2}	-1.599×10^{-3}	1.355×10^{-4}	-2.317×10^{-6}	-1.113×10^{-8}	0	0.1–23
$NaBr \cdot 2H_2O$[c]	0.9996	-3.116×10^{-2}	-2.112×10^{-3}	-9.347×10^{-5}	2.000×10^{-5}	-5.47×10^{-7}	0	0.1–2.(

[a] Selected data from Cohen et al., 1987; Na, 1994; and Chiou, 1994. [b] The molality m is based on the hydrate mol/kg of free wate
[c] The molality m is based on the anhydrous mol/kg of total water.

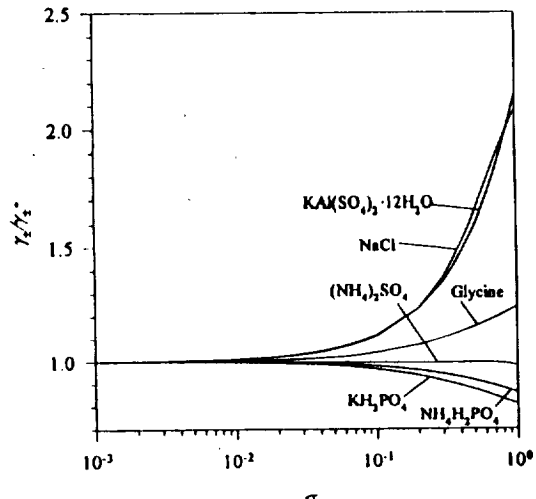

Figure 1. Mean ionic solute activity coefficient ratio versus dimensionless supersaturation (molality-based).

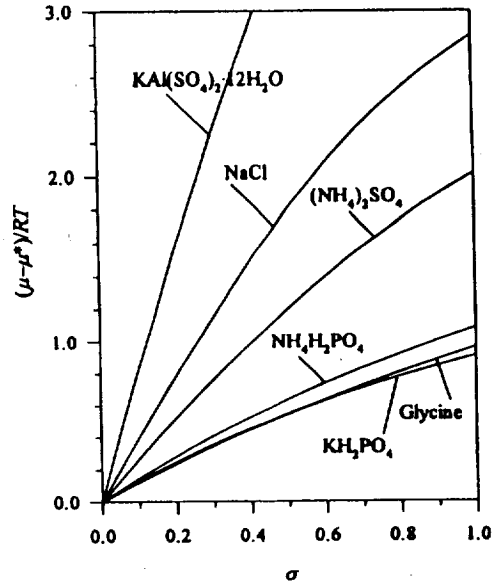

Figure 2. Fundamental driving forces calculated as function dimensionless supersaturation (molality-based).

Na (1993) were used to calculate the solute activity as a function of concentration. Additional measurements of the water activity for supersaturated $NH_4H_2PO_4$, KH_2PO_4, and $KAl(SO_4)_2 \cdot 12H_2O$ solutions were carried out in our laboratory using the spherical void electrodynamic levitator trap. Details of the experiments can be found elsewhere (Na, 1993). The water activity expressed as a polynomial function of molality (listed in Table 1) was used in the numerical calculation of eq 5 to acquire the activity coefficient ratio as a function of concentration.

The calculated ratio, $\gamma_\pm/\gamma_\pm^*$ is plotted as a function of dimensionless supersaturation, σ (molality-based), in Figure 1. The ratio remains very close to unity up to the supersaturation degree of $\sigma = 0.01$; as σ increases, the activity coefficient deviates either positively (for NaCl, $KAl(SO_4)_2 \cdot 12H_2O$, glycine) or negatively (for $NH_4H_2PO_4$, KH_2PO_4, $(NH_4)_2SO_4$) from that of the saturated solution. The biggest deviation of the activity coefficient is found for the solutions of NaCl and $KAl(SO_4)_2 \cdot 12H_2O$ and the least deviation for $(NH_4)_2SO_4$.

Figure 2 shows the calculated fundamental driving force, $\Delta\mu/RT$ ($=\nu \ln(a_\pm/a_\pm^*)$), as a function of σ. The big differences between $\Delta\mu/RT$ and σ for $KAl(SO_4)_2 \cdot 12H_2O$ and NaCl are due to relatively large deviations of $\gamma_\pm$ from $\gamma_\pm^*$ and the values of ν ($\nu = 4$ for $KAl(SO_4)_2 \cdot 12H_2O$, $\nu = 2$ for NaCl). For $(NH_4)_2SO_4$ which had a relatively small deviation of $\gamma_\pm/\gamma_\pm^*$ in all ranges of σ, the difference is mainly due to the value of $\nu = 3$. Although it is not apparent from the plots, all the curves have a linear section with slope ν in the region of σ below 0.01. The leveling down curvature at high σ (above 0.5) is due mainly to the fact that $\ln(\sigma + 1)$ becomes relatively smaller than σ as σ increases.

Parts a–d of Figure 3 show the experimental d points of the growth rate versus σ and versus $\Delta\mu/RT$. The kinetic parameters for the rate expressions of t forms in eqs 7 and 8 were determined from line regressions of the logarithmic plots. The evaluate kinetic parameters are listed in Table 2. It should b noted that the kinetic parameters k_r and n are good only the experimental range of σ indicated in the tal whereas k_r' and n' are valid for all ranges of supersa ration. The values of n and n' are close for the d measured at the range of very low σ (less than 0.01) which the fundamental driving force and concentrat driving force remain more or less proportional to e other. For example, the values of n and n' are alm identical for $(NH_4)_2SO_4$ (measure at $\sigma < 0.007$) and N (measured at $\sigma < 0.004$). On the other hand, KH_2 (measured at $0.1 < \sigma < 0.2$) shows much different n n'.

The solid lines (extrapolated from the growth data with respect to $\Delta\mu/RT$) shown in Figure 3 represent the true kinetics of crystal growth over ranges of the driving force. The true rates of gro determined from the fundamental driving force v plotted against σ (broken solid lines). These are t growth rates that would be measured in kinetic exp ments conducted over a wide range of σ. The p clearly show that different values of the kinetic par eters k_r and n would be obtained from experim conducted at different ranges of supersaturation. T dotted lines, which were extrapolated from the gro

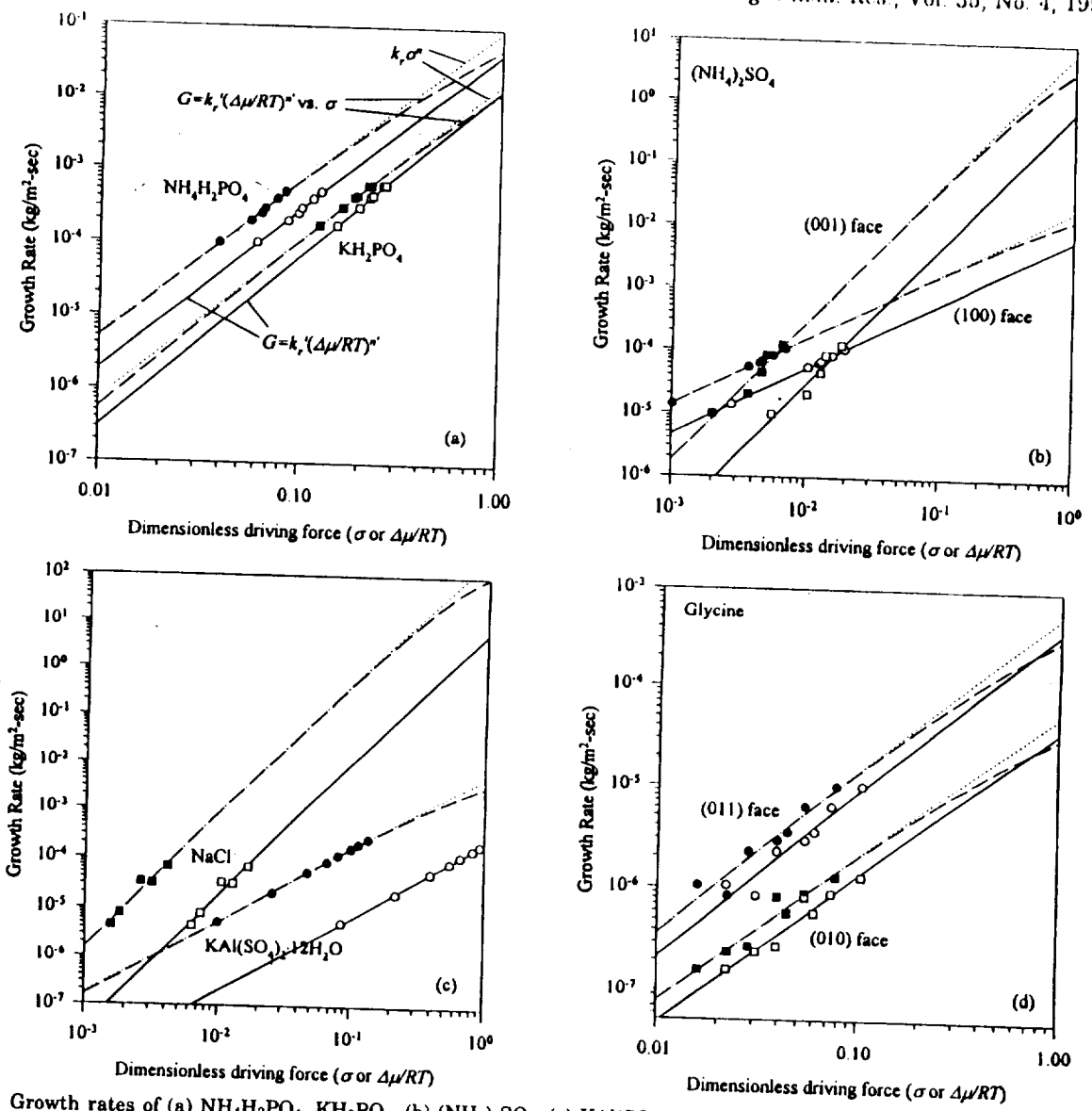

Figure 3. Growth rates of (a) $NH_4H_2PO_4$, KH_2PO_4, (b) $(NH_4)_2SO_4$, (c) $KAl(SO_4)_2{\cdot}12H_2O$, NaCl at 25 °C, and (d) glycine at 20 °C as functions of dimensionless driving force σ (filled symbols) or $\Delta\mu/RT$ (hollow symbols). The straight solid lines are the calculated rates from the expression $G = k_r'(\Delta\mu/RT)^{n'}$. The broken solid lines are the same rates plotted against σ. The dotted lines represent the rates based on $G = k_r\sigma^n$. (Experimental data adapted from Mullin and Amatavivadhana, 1967; Mullin et al., 1970; Mullin and Garside, 1967a,b; Rumford and Bain, 1960; Li and Rodríguez-Hornedo, 1992.)

Table 2. Kinetic Parameters of Crystal Growth Evaluated from Experimental Data

compound	experimental method	ref	σ range of experiments	$G = k_r\sigma^n$		$G = k_r'(\Delta\mu/RT)^{n'}$	
				k_r	n	k_r'	n'
$NH_4H_2PO_4$	single crystal face growth measurements using microscope	Mullin and Amatavivadhana, 1967	0.04–0.08	9.1×10^{-2}	2.12	4.3×10^{-2}	2.18
KH_2PO_4	single crystal face growth measurements using microscope	Mullin and Amatavivadhana, 1967	0.1–0.2	1.6×10^{-2}	2.18	1.3×10^{-2}	2.32
$(NH_4)_2SO_4$							
(100) face	single crystal face growth measurements using microscope	Mullin et al., 1970	0.001–0.007	1.9×10^{-2}	1.05	6.6×10^{-3}	1.05
(001) face			0.002–0.007	6.9	2.20	7.3×10^{-1}	2.20
$KAl(SO_4)_2{\cdot}12H_2O$	fluidized-bed crystallizer	Mullin and Garside, 1967a,b	0.01–0.13	5.3×10^{-3}	1.50	2.3×10^{-4}	1.53
NaCl	fluidized-bed crystallizer	Rumford and Bain, 1960	0.001–0.004	2.6×10^{2}	2.74	5.7	2.74
glycine							
(011) face	single crystal face growth measurements using microscope	Li and Rodríguez-Hornedo, 1992	0.01–0.08	5.4×10^{-4}	1.58	3.6×10^{-4}	1.61
(010) face			0.01–0.08	5.3×10^{-5}	1.41	3.7×10^{-5}	1.44

rate data with respect to σ, are included only to illustrate the inadequacy of the rate expression based on σ (eq 7).

In general, the order n obtained from the experimental data of low σ (<0.01) can be considered a close approximation of the true kinetic order n'. We are interested in how n (determined from experiment) deviates from n' as σ increases. The true growth rate G can be expressed as:

$$G = k'(\Delta\mu/RT)^{n'} = k(\sigma)\,\sigma^{n(\sigma)} \qquad (13)$$

where k' and n' are constant, but $k(\sigma)$ and $n(\sigma)$ are

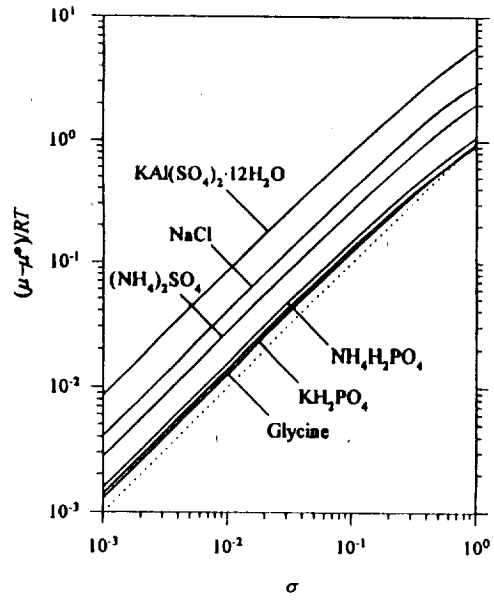

Figure 4. Fundamental driving force versus dimensionless supersaturation based on molality.

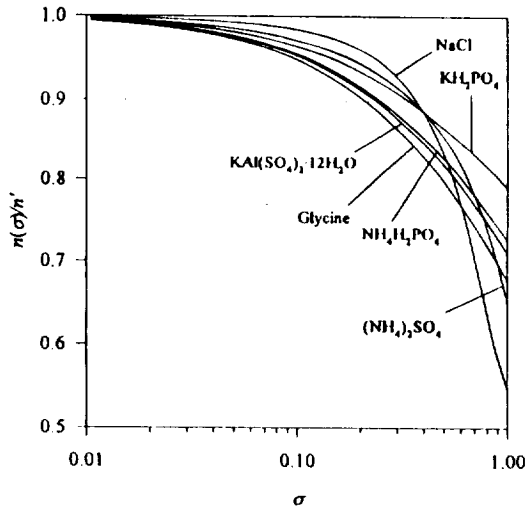

Figure 5. $n(\sigma)/n'$ determined from the tangent lines of the plots in Figure 4 versus σ.

changing functions of σ. Taking the logarithm of both sides produces:

$$\log k' + n' \log(\Delta\mu/RT) = \log k(\sigma) + n(\sigma) \log \sigma \quad (14)$$

Equation 14 indicates that $d(\log(\Delta\mu/RT))/d(\log \sigma)$ is equal to the ratio of the kinetic orders, $n(\sigma)/n'$. Therefore, in the logarithmic plots of $\Delta\mu/RT$ versus σ (shown in Figure 4), slopes of the tangent lines at varying σ should be equal to $n(\sigma)/n'$. It is easily seen from the figure that the plots have the tangent lines with slopes very close to unity when $\sigma < 0.01$, and the slopes decrease with increasing σ. The ratio $n(\sigma)/n'$ determined from the slopes with varying σ is plotted in Figure 5. In all of the crystallizing systems considered here, $n(\sigma)$ is within 5% below n' in the range of σ below 0.1. As indicated in the figure, the range of σ at which $n(\sigma)/n' < 0.9$ can be considered as the concentration region where $n(\sigma)$ significantly deviates from n'.

b. Diffusion-Limited Crystallization. The overall growth rates of $KAl(SO_4)_2 \cdot 12H_2O$ measured by Mullin and Garside (1968) at 32 °C were investigated in terms of the fundamental driving force using the boundary layer diffusion model described earlier. Separate experimental data (Mullin and Garside, 1967a,b) were used to evaluate the kinetic parameters for the surface integration rates and the mass-transfer coefficient with respect to σ and $\Delta\mu/RT$. The fundamental driving force $\Delta\mu/RT$ was calculated from the activity coefficient function determined at 25 °C. Using the activity coefficient function at 25 °C for the data at 32 °C can be justified by the fact that the activity coefficients of many binary mixtures have a very small dependence on temperature in a moderate temperature range (Prausnitz et al., 1986).

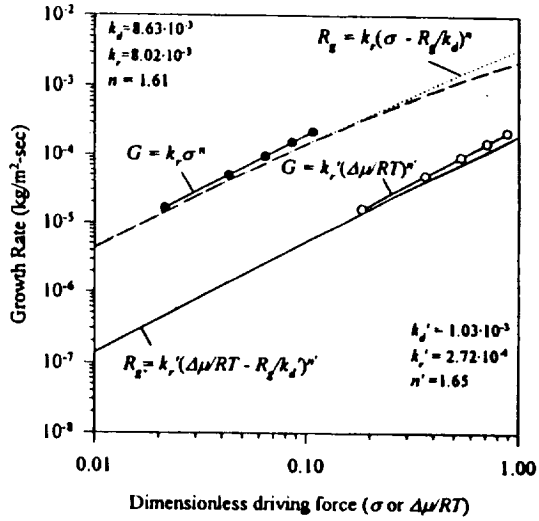

Figure 6. Overall growth rate of $KAl(SO_4)_2 \cdot 12H_2O$ at 32 °C (diffusion-limited growth) as functions of dimensionless driving force σ or $\Delta\mu/RT$. (mean crystal size = 750 μm; solution velocity = 0.05m/s). The data points represent the surface integration rates at 32 °C with respect to σ (filled circles) or $\Delta\mu/RT$ (hollow circles). (Experimental data adapted from Mullin and Garside, 1968.)

Figure 6 shows numerically calculated overall growth rates using eq 12 plotted against $\Delta\mu/RT$ (solid line) and σ (broken solid line). The experimental data of the surface integration rates are also shown in the figure. The false growth rates determined from eq 10 were also plotted as a function of σ for comparison. It shows that the rates determined from eq 10 would be misleading in the range of σ above 0.1.

Kinetics of Nucleation. The primary nucleation rates of KCl, KBr, NH_4Cl, $(NH_4)_2SO_4$, and $NaBr \cdot 2H_2O$ at 30 °C are reported by Nývlt et al. (1970). The kinetic parameters had been determined by the measurements of the metastable zone width. The nucleation parameters determined by this method are known to give only "apparent" kinetics because growth of critical nuclei to visible size is neglected. Nevertheless, the resulting parameters provide an effective nucleation rate not much different from the real kinetics of nucleation in many cases and close enough for engineering purposes (Nývlt et al., 1985). Furthermore, since our purpose is simply to illustrate the effects of using the fundamental driving force on nucleation kinetics, we are presenting the analysis using these parameters.

The nucleation rate can be written as:

$$J = k_n \sigma^m \quad (15)$$

which is valid only in the experimental σ range, and

$$J = k_n'(\Delta\mu/RT)^{m'} \quad (16)$$

which is the fundamental nucleation kinetics valid over a wider range of concentration.

Table 3. Kinetic Parameters of Nucleation of Various Compounds

compound	range of σ measured	$G = k_n\sigma^m$ order m	$G = k_n'(\Delta\mu/RT)^{m'}$ order m'
KBr	0.01–0.04	2.49	2.51
KCl	0.01–0.02	5.98	5.99
$NaBr{\cdot}2H_2O$	0.03–0.07	2.11	2.14
NH_4Cl	0.01–0.02	4.57	4.61
$(NH_4)_2SO_4$	0.01–0.02	4.85	4.87

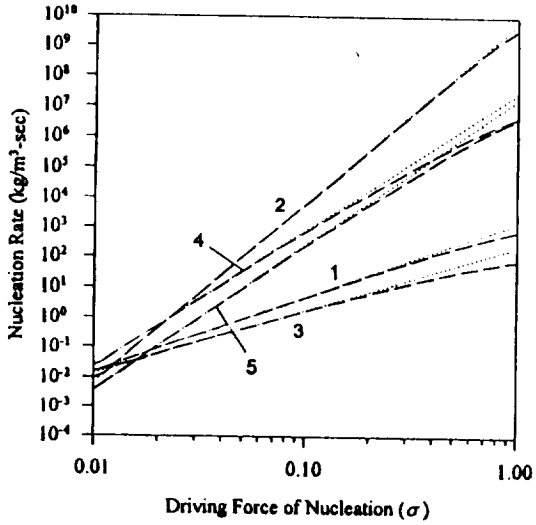

Figure 7. Nucleation rates of KBr (plots 1), KCl (plots 2), $NaBr{\cdot}2H_2O$ (plots 3), NH_4Cl (plots 4), and $(NH_4)_2SO_4$ (plots 5) at 30 °C as functions of σ. (Experimental data adapted from Nývlt et al., 1970.)

After converting the supersaturation data to be in the unit of molality, the nucleation parameters were re-evaluated in terms of σ and $\Delta\mu/RT$. The nucleation rates were expressed in the unit of kg of crystal/(m^3 of solution·s). The comparisons of the orders m and m' are presented in Table 3.

Figure 7 shows the nucleation rates versus the dimensionless driving force σ. The extrapolated dotted lines representing eq 15 seem to coincide with the true nucleation rates depicted by eq 16 (broken solid lines) in the range of σ below 0.1, but the deviation increases with increasing σ.

Conclusions

Kinetics of crystal growth and nucleation of various salts were investigated in terms of the fundamental driving force of crystallization based on the chemical potential difference. The chemical potentials of supersaturated solutions were calculated as a function of concentration from the activity of supersaturated solutions. The kinetic expressions based on the chemical potential difference are thermodynamically exact representations of the true kinetics of crystallization. The commonly used kinetic expressions based on the concentration difference are in significant error at the high supersaturation range, in which many crystallization processes are commonly operated.

Acknowledgment

Support of this work through NSF Grant CTS-9020233 and NASA Grant NA68-960 is gratefully acknowledged.

Nomenclature

a = activity of solute
$a_\pm$ = mean ionic activity of solute
a_w = activity of water in aqueous solution
c = concentration of solute in any unit
c_i = concentration of solute at the interface between the solution and the boundary layer
G = crystal growth rate (surface integration), kg/m^2·s
J = crystal nucleation rate, kg/m^3·s
k = crystallization rate constant, kg/m^2·s
k' = crystallization rate constant with respect to $\Delta\mu/RT$, kg/m^2·s
k_d = mass-transfer diffusion coefficient, kg/m^2·s
k_n = nucleation rate constant, kg/m^3·s
k_n' = nucleation rate constant with respect to $\Delta\mu/RT$, kg/m^3·s
k_r = surface integration rate constant, kg/m^2·s
k_r' = surface integration rate constant with respect to $\Delta\mu/RT$, kg/m^2·s
m = molal concentration of solute, mol/kg of water
m = order of crystal nucleation rate expression based on σ
m' = order of crystal nucleation rate expression based on $\Delta\mu/RT$
MW_w = molecular weight of water, g/mol
n = order of crystal growth rate expression based on σ
n' = order of crystal growth rate expression based on $\Delta\mu/RT$
R = gas constant, J/mol·K
R_g = overall rate of diffusion-limited crystal growth, kg/m^2·s
T = temperature, K
ϕ = osmotic coefficient
$\gamma_\pm$ = mean ionic activity coefficient
μ = chemical potential, J
μ_i = chemical potential at the interface between the solution and the boundary layer, J
$\Delta\mu$ = chemical potential difference between supersaturated and saturated solution, $\mu - \mu^*$, J
ν = number of moles of ions formed from 1 mol of electrolyte
σ = relative supersaturation, $(c - c^*)/c^*$ or $(m - m^*)m^*$
* = of saturated solution

Literature Cited

Chiou, J. M. A comparison of the Use of Chemical Potential and Concentration on Crystal Growth Kinetics. Master Thesis; Polytechnic University: Brooklyn, NY, 1994.

Cohen, M. D.; Flagen, R. C.; Seinfeld, J. H. Studies of Concentrated Electrolyte Solutions Using the Electrodynamic Balance. 1. Water Activities for Single-Electrolyte Solutions. *J. Phys. Chem.* **1987**, *91*, 4563–4574.

Li, L.; Rodríguez-Hornedo, N. Growth Kinetics and Mechanism of Glycine Crystals. *J. Cryst. Growth* **1992**, *121*, 33–38.

Mullin, J. W.; Amatavivadhana, A. Growth Kinetics of Ammonium– and Potassium–Dihydrogen Phosphate Crystals. *J. Appl. Chem.* **1967**, *17*, 151–156.

Mullin, J. W.; Garside, J. The Crystallization of Aluminium Potassium Sulphate: a Study in the Assessment of Crystallizer Design Data Part I: Single Crystal Growth Rates. *Trans. Inst. Chem. Eng.* **1967a**, *45*, T285–290.

Mullin, J. W.; Garside, J. The Crystallization of Aluminium Potassium Sulphate: a Study in the Assessment of Crystallizer Design Data Part II: Growth in a Fluidized Bed Crystallizer. *Trans. Inst. Chem. Eng.* **1967b**, *45*, T291–295.

Mullin, J. W.; Garside, J. The Crystallization of Aluminium Potassium Sulphate: a Study in the Assessment of Crystallizer Design Data Part III. Growth and Dissolution Rates. *Trans. Inst. Chem. Eng.* **1968**, *46*, T11–18.

Mullin, J. W.; Söhnel, O. Expressions of Supersaturation in Crystallization Studies. *Chem. Eng. Sci.* **1977**, *32*, 683–686.

Mullin, J. W.; Chakraborty, M.; Mehta, K. Nucleation and Growth of Ammonium Sulphate Crystals from Aqueous Solution. *J. Appl. Chem.* **1970**, *20*, 367–371.

Na, H. S. Cluster Formation and Nucleation in Highly Supersaturated Droplets. Ph.D. Thesis, Polytechnic University: Brooklyn, NY, 1993.

Na, H. S.; Arnold, S.; Myerson, A. S. Cluster Formation in Highly Supersaturated Solution Droplets. *J. Cryst. Growth* **1994**, *139*, 104–112.

Na, H. S.; Arnold, S.; Myerson, A. S. Water Activity in Supersaturated Aqueous Solutions of Organic Solutes. *J. Cryst. Growth* **1995**, *149*, 229–235.

Nývlt, J.; Rychlý, R.; Gottfried, J.; Wurzelová, J. Metastable Zone-Width of Some Aqueous Solutions. *J. Cryst. Growth* **1970**, *6*, 151–162.

Nývlt, J.; Söhnel, O.; Matuchová, M.; Broul, M. The Kinetics of Industrial Crystallization. *Chemical Engineering Monographs*; Elsevier: New York, 1985; Vol. 19.

Prausnitz, J. M.; Lichenthaler, R. N.; de Azevedo, E. G. *Molecular Thermodynamics of Fluid-Phase Equilibria*; Prentice-Hall: Englewood Cliffs, NJ, 1986.

Robinson, R. A.; Stokes, R. H. *Electrolyte Solutions*, 2nd ed.; Butterworths: London, 1959.

Rumford, F.; Bain, J. The Controlled Crystallisation of Sodium Chloride. *Trans. Inst. Chem. Eng.* **1960**, *38*, 10–20.

Söhnel, O.; Mullin, J. W. Expressions of Supersaturation ... Systems Containing Hydrates, Partially Dissociated Electrol... and Mixtures of Electrolytes. *Chem. Eng. Sci.* **1978**, *33*, 15...–1538.

Received for review June 1, 1...
Revised manuscript received October 4, 1...
Accepted October 16, 19...

IE9503...

• Abstract published in *Advance ACS Abstracts*, Febr... 15, 1996.